

Comparison between simplified approach and CFD & Propagation tool for sonic boom estimation

Original

Comparison between simplified approach and CFD & Propagation tool for sonic boom estimation / Graziani, S., Viola, N., Petrosino, F., Jäschke, J.. - (2023). (AIAA Aviation 2023 Forum San Diego, CA (USA) 12-16 June 2023) [10.2514/6.2023-4166].

Availability:

This version is available at: 11583/2988089 since: 2025-09-02T14:12:53Z

Publisher:

AIAA

Published

DOI:10.2514/6.2023-4166

Terms of use:

This article is made available under terms and conditions as specified in the corresponding bibliographic description in the repository

Publisher copyright

AIAA preprint/submitted version e/o postprint/Author's Accepted Manuscript

(Article begins on next page)

Comparison between simplified approach and CFD & Propagation tool for sonic boom estimation

S. Graziani*, N. Viola.†
Politecnico di Torino, Torino, Italy, 10129

F. Petrosino‡
CIRA, Capua, Italy, 81043

J. Jäschke§
Hamburg University of Technology, Hamburg, Germany, 21073

The following paper compares results obtained through a simplifying methodology that can be used at the conceptual design phase with results obtained through CFD and then propagation code for ground signature. The application of state-of-the-art models for future supersonic aircraft is discussed within the paper and solutions to overcome these limitations will be presented. Validation using CFD techniques and propagation tools is necessary to accurately define which design and flight condition characteristics most affect noise generation and propagation, as well as to integrate and improve existing methods in the literature with new formulations to estimate sonic boom at an early stage of design. The following workflow was validated for an aircraft with a Concorde-like configuration within the EU-funded MORE&LESS project.

I. Nomenclature

$A(x)$	=	Equivalent area due to volume
$B(x)$	=	Equivalent area due to lift
$A_e(x)$	=	Total effective area of the aircraft
h_e	=	aircraft altitude above ground
K_d	=	ray-path distance factor direction
K_s	=	Aircraft shape factor
l_e	=	Effective length of the aircraft
Δp	=	Incremental pressure due to sonic boom
Δt	=	Time increment
γ	=	Flight path angle
θ	=	Ray- path azimuth angle
i	=	time index during navigation
j	=	waypoint index
K	=	trailing-edge (TE) nondimensional angular deflection rate
PLdB	=	Perceived Level of loudness in dB

II. Introduction and background

CIVIL aviation over the past century has evolved very rapidly, changing how we live and work, as well as connecting the world. Today, traveling thousands of miles in a few hours is much easier, safer, and more affordable than it was a century ago. However, following the first generation of civil supersonic aircraft originated and developed during the 1960s, the supersonic regime remains confined purely to military purposes, and with the growing effort to achieve environmental sustainability of the industry, the sustainability of civil supersonic aircraft has still to be guaranteed.

*PhD Student, Politecnico di Torino, Italy, samuele.graziani@polito.it

†Associate Professor, Politecnico di Torino, Italy, nicole.viola@polito.it

‡Senior Researcher, Italian Aerospace Research Center, f.petrosino@cira.it, AIAA Member

§PhD student, Hamburg University of Technology, jacob.jaeschke@tuhh.de.

The EU-funded H2020 MORE&LESS project aims to investigate the environmental impact of supersonic aircraft through multi-fidelity simulations and test campaigns in order to lay the groundwork for creating multidisciplinary holistic framework to evaluation the future supersonic aircraft, trajectories, and operations that can reduce their environmental impact. The project aims to analyze the flight regime between Mach 2 and Mach 5 by evaluating different configurations, and new propulsion technologies and assessing alternative fuels such as Biofuel and Liquid Hydrogen.

Due to the renewed interest in environmentally sustainable supersonic aircraft, there has been growing activity in the development of new concepts for supersonic aircraft in recent decades. Following the first flight tests on the Concorde, a global debate started about the environmental concerns of this type of aircraft and the disturbance they can cause to citizens on the ground. The second generation of supersonic aircraft shall aim to define new standards for the flight over the land for both sonic boom annoyance during the cruise mission phase and for the LTO noise in the proximity of the airports. Moreover, new routines should be developed that can be effectively integrated into a workflow to address these concerns early in the design.

The main purpose during the conceptual design phase concerns the study of the technical feasibility of the various configurations to reduce the effort required in the subsequent parts of the detailed design. However, in this phase of the project, there is also the need to have simulations of performance, trajectories, and aerodynamic analyzes to evaluate all the improvements to the configuration. For the new generation of supersonic aircraft, environmental sustainability, and noise reduction are requirements that must be properly integrated into the project workflow from the conceptual design stages since they bring constraints to the development of the configuration itself.

Following the objective of the MORE&LESS project, an integrated workflow to support the conceptual design phase of the new generation of supersonic aircraft was developed in figure 1. It considers, together with the other requirements of performance, aerodynamics, and trajectory, also the requirements concerning noise and verification within initial assessment studies. The integration of new routines begins with the consideration of new environmental targets that will have to be defined and limitations for supersonic aircraft in continental areas, and from these new standards, an iterative cycle is developed that leads to the development of a configuration that meets the requirements. However, as for the noise created by the sonic boom, it is known that any object moving faster than the local speed of sound creates a shock wave system that propagates through the atmosphere and can eventually reach the ground. At a great distance from the aircraft, this wave system can coalesce and increase the noise level perceived on the ground, causing a higher annoyance level to the population. This wave system is a characteristic of the entire mission profile in a supersonic regime and moves at the same speed as the aircraft. Sonic boom minimization techniques are of enormous importance because, with current restrictions, it is impossible to fly over continents in a supersonic regime for civilian purposes.

The first procedure for shock formation was studied by Whitham [1] which corrected the linearized theory including the local variation of the speed of sound and formation of shocks. Most early studies were conducted considering a standard atmosphere or a uniform, isothermal atmospheres such as those of George and Seebass [2] [3] [4]. The effect of a real atmosphere was first studied by Hayes [5] and then taken up by Pierce and Maglieri [6]. The most widely used methods are set out by Plotkin [7]. Besides these methods, which are quite complex and require a great amount of computing power, simplified models have also been developed to approximate the Whitham F function. However, accurate results could also be obtained through simplified methodologies found in the literature and derived from studies based on linearized supersonic flow theory.

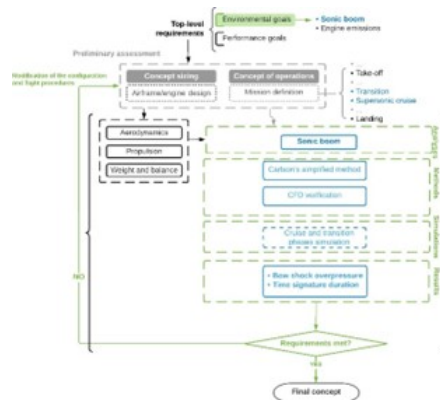


Fig. 1 Workflow for the second generation of Supersonic Aircraft

Within this paper is a comparison between flight conditions studied through Carlson’s simplified method [8] and more detailed simulations done through CFD and propagation tools. The main advantage of Carlson’s theory is that it allows sensitivity analyses to be evaluated as flight parameters change. Another simplifying method that can be used at the conceptual design stage is the one formulated by Plotkin [9], who presents a method for evaluating the sonic boom from an aircraft maneuvering in an arbitrary, windless, and horizontally stratified atmosphere. However, it is known that the parameters that most influence the level of sonic boom intensity are related to the aircraft’s flight altitude, Mach number at cruise, wind, and weight in that flight condition. Moreover, the shape of the configuration is another factor for the noise level produced. For the next generation of supersonic aircraft, there is a need to include a design, that minimizes the noise during cruise flight, already from the initial design phase.

As a case study for this paper, a Concorde-like configuration was used with similar performance and geometric characteristics to the original aircraft, which is currently a case study within the MORE&LESS project. To be sustainable, the vehicle is studied using biofuel as a propellant.

III. Case Study

One of the reference aircraft within the MORE&LESS project was used as a case study. In particular, the configuration chosen reproduces a Concorde-like aircraft, with geometric and performance characteristics very similar to the reference aircraft. In particular, for the sizing was used the internal design tool at the Politecnico di Torino. The task was to define a nominal configuration of an aircraft at Mach 2 having biofuel as the propellant, starting from the high-level requirements of the Concorde Design parameters including cruise Mach, weight, volume, range, and payload. The impact of biofuel on the design configuration of the case study is investigated as well. In particular, the design and operational requirement coming from Concorde are:

- Range ≥ 7200 km
- Passenger ≥ 120
- MTOW ≤ 200000 kg
- Cruise @ Mach 2
- Same configuration of Concorde

On the other hand, the main novelties introduced are:

- Use of biofuels
- More efficient propulsive plant

Data	MORE&LESS CS-1a
Design GTO Mass [kg]	179849
OEW [kg]	79460
Design fuel weight [kg]	85289
Design Payload weight	15200
Wing Surface [m ²]	358
Aircraft Length [m]	61.7
Wingspan [m]	25.6
Performance	
Design Range [km]	6500
Cruise Altitude [m]	18000
Thrust to weight ratio (dry at TO)	0.4
Wing Loading [kg/m ²]	494
Lift over drag ratio	7
Max Mach	2.2
Required Runway Length [m]	3400

Table 1 CS-1a geometric and performance data

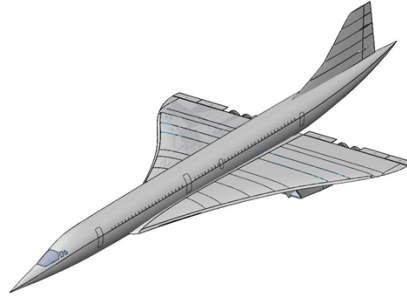


Fig. 2 CS-1a reference aircraft

Based on the aerodynamic and propulsive database carried out on the aircraft, a mission analysis was carried out to verify that it complied with the requirements imposed in the definition phase. From the results of the mission analysis, some characteristic points in the supersonic regime have been selected to study the disturbance given by the sonic boom. The aircraft can cover a mission profile that falls within the requirements imposed in the design phase and a generic long-haul route is considered, for a total range of 6500 km. The mission is feasible, with a total duration of almost four hours.

As previously mentioned, the flight conditions that have been studied by the CFD are some of those found by the mission profile developed through the ASTOS software.

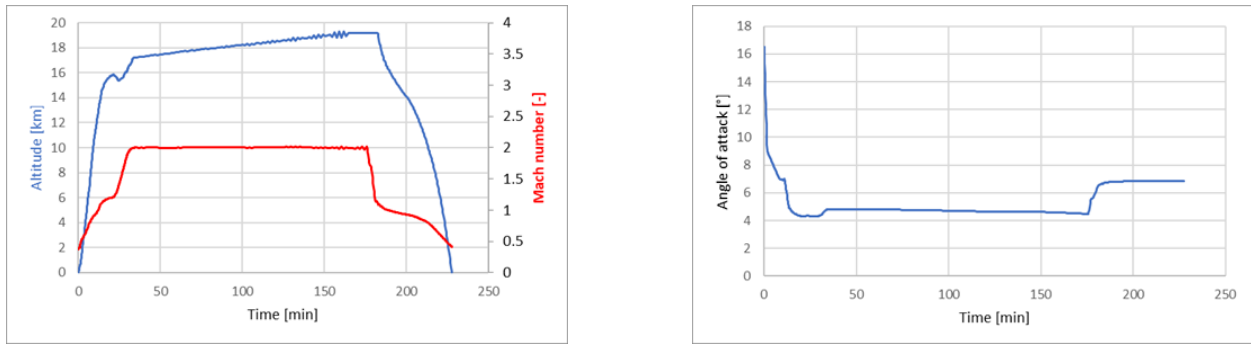


Fig. 3 CS-1a Mission profile and Angle of Attack evaluation

IV. Sonic Boom Simplified Prediction method

For the preliminary study within simplifying methods, it was decided to use Carlson's one [8], which can assess the value of bow shock over-pressure and time signature duration from the early stages of conceptual design. Unlike other approaches, or CFD itself, this methodology does not require a large amount of data and applies to all supersonic aircraft in stationary flight or slight climb/descent phases up to about 76 km altitude.

However, the method itself has many limitations for applications other than conceptual design and cross-check; in fact, the method is only valid for N-wave waves (a compression followed by a linear expansion to pressure below ambient and finally a second shock to restore the value of pressure), in addition to the fact that it considers only a windless atmosphere and stationary conditions. Normally, common supersonic aircraft used to have this typology of pressure signatures, at least for the bow shock and the positive portion of the signature.

The simplification process consists of the evaluation of the Whitham F function, which is approximated to a constant called aircraft shape factor, which is a function of the physical, environmental, and geometric characteristics of the vehicle. For some types of them, within the Carlson method, there are already some graphs for the evaluation of the aircraft shape factor, which allow a very rapid assessment of the level of over-pressure and time signature duration.

The first step in determining bow shock over-pressure and time signature duration with this methodology is the evaluation of the aircraft shape factor of the aircraft itself, regarding the flight conditions like cruise Mach number and effective altitude. Afterwards, it is possible to derive the values of the ray path distance factor, time signature factor, and

pressure amplification factor. The third and final step for this first phase of the methodology is the application of the bow shock over-pressure formulation in Equation 1 and time signature duration in Equation 2:

$$\Delta p_{max} = K_P \cdot K_R \cdot \sqrt{p_v \cdot p_g} \cdot (M^2 - 1)^{\frac{1}{8}} \cdot h_e^{-\frac{3}{4}} \cdot l^{\frac{3}{4}} \cdot K_S \quad (1)$$

Here, K_P is the pressure amplification factor, K_R is the reflection factor that was assumed equal to 2.0, p_v is the atmospheric pressure at aircraft flight altitude, p_g is the value of atmospheric pressure at ground, h_e is the effective altitude and finally K_S is the aircraft shape factor.

$$\Delta t = K_t \cdot \frac{3.42}{a_v} \cdot \frac{M}{(M^2 - 1)^{\frac{3}{8}}} \cdot h_e^{\frac{1}{4}} \cdot l^{\frac{3}{4}} \cdot K_S \quad (2)$$

Here, K_t is the signature duration factor, a_v is the speed of sound at aircraft altitude.

The procedure for the calculation of the shape factor parameter in case the aircraft is not covered by specific graphs for the shape factor consists of the evaluation of a series of parameters. The first is the definition of the equivalent area due to volume, which would be defined as the cross-sectional area normal to the Mach cone. However, the methodology provides for simplification, considering only areas that are normal to the flight path, unless the angle of attack is very large. There is a loss of accuracy since for blunt shapes or high supersonic speeds, the normal areas are more appropriate. If it is known, the area of the air stream tube entering the engine inlet should be removed from the calculation.

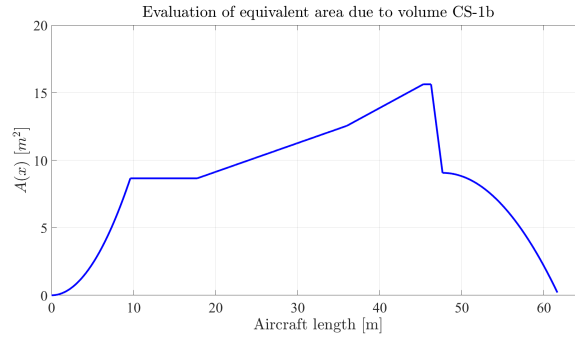


Fig. 4 Equivalent area due to volume CS-1a

Furthermore, the second step consists in the definition of the equivalent area due to lift, which is approximated with the plan-form area distribution and could be written as:

$$B(x) = \frac{\sqrt{M^2 - 1} \cdot W \cdot \cos \gamma \cdot \cos \theta}{1.4 \cdot p_v \cdot M^2 \cdot S} \int_0^x b(x) dx \quad (3)$$

Here, W is the aircraft weight, γ is the flight path angle, θ is ray path azimuth angle, S is the aircraft plan-form area and finally $b(x)$ is the local span of the aircraft along the longitudinal axis. The lifting force which influences the sonic boom is defined by an aircraft weight component that is normal to the flight path and directed along the initial ray-path azimuth angle θ .

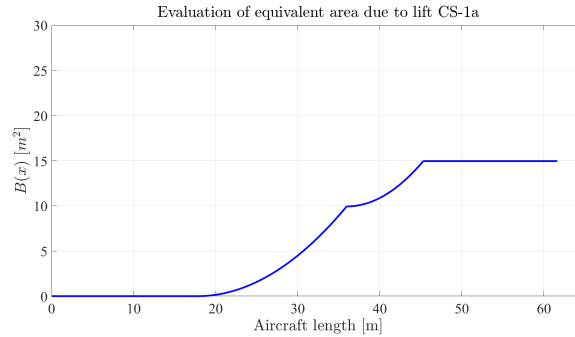


Fig. 5 Equivalent area due to lift CS-1a

The third step consists in the combination of the two areas previously obtained to obtain the total effective area of the aircraft. Through the following charts, it is possible to obtain the maximum effective area $A_{e,maxi}$, its location, that is called effective length l_e and the effective area $A_{e,1}$ that is necessary for the calculation of the shape factor.

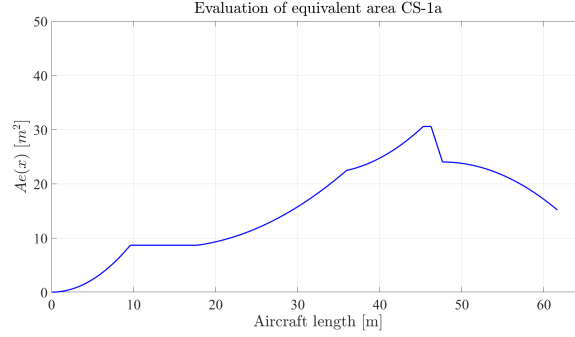


Fig. 6 Total effective area due to lift CS-1a

It was first assumed that the ray path curvature and the value of over-pressure due to atmospheric effects depended solely on the initial inclination of the ray path generated with respect to the ground plane and ray path distance calculated perpendicular to the flight path of the aircraft. A measure of ray path inclination is given by the number of Mach in level flight, having the same flight path angle in the flight track plane, and this is named actual Mach number. The effective altitude is just the distance measured perpendicular to the aircraft flight path.

The effective Mach number could be written in equation 4, while the effective altitude is evaluated in equation 6:

$$M_e = \frac{1}{\sin(\gamma + \cot^{-1}(\sqrt{M^2 - 1}))} \quad (4)$$

The component of distance in direction of the aircraft ground track could be evaluated as:

$$d_x = K_d \cdot \left(\frac{h}{\sqrt{M_e^2 - 1}} \right) \quad (5)$$

Finally, it is possible to evaluate the effective altitude having all of these parameters:

$$h_e = h \cdot \cos \gamma + d_x \cdot \sin \gamma \quad (6)$$

The set of atmospheric parameters was characterized by interpolating polynomial equations. Within Carlson's methodology, there are numerous graphs related to simplified atmospheric parameters such as the cutoff Mach number, the ray path distance factor, the pressure amplification factor and the signature duration factor.

V. Higher Fidelity Approach

To evaluate the accuracy of the simplified methodology, a higher-fidelity study is conducted for comparison. The higher-fidelity study consists of two steps. Firstly, a computational fluid dynamics (CFD) simulation is carried out to model the shock waves generated in the near field of the supersonic aircraft. Secondly, a dedicated propagation tool is used to simulate the propagation of the shock waves through the atmosphere towards the ground, taking into account the nonlinear aspects of sound propagation and the inhomogeneities of the atmospheric fluid.

A. Near-field sonic boom CFD simulation

Sonic boom prediction involves complex physical phenomena, aerodynamic instabilities, pressure disturbances and high-speed aerodynamic flows. Numerical simulation approach could produce an accurate evaluation of the near-field aerodynamic pressure perturbations, that cause the sonic boom. In order to accurately represent the non linear interactions (energy transfers) inside the shock structure and generate the right sonic boom signature, numerical discretization and precision of advective terms are crucial. A appropriate grid resolution is linked to a filter that is implicitly defined, which might change the frequency content of the numerical solution.

Since 2014, NASA promoted the Sonic Boom Prediction Workshop[10][11][12], which aim to assess numerical methods to predict sonic boom. The results of workshops provide guidance for accurate computational forecasting of noise generated by supersonic aircraft. In particular, the choice of mesh strategies, in terms of refinement and adaption approach, permitting the proper tracking of discontinuity needs specific effort. In this work was used the open-source code SU2 Multiphysics Simulation and Design Software[13], that includes several numerical schemes, turbulence models and boundary conditions to cover different fluid-dynamic problems. The near-field sonic boom simulation was solved using an Euler approach, without turbulence model activation, and selecting the HLLC (Harten-Lax-van Leer-Contact) numerical scheme[14]. The HLLC scheme is a modification of the HLL scheme whereby the missing contact and shear waves in the Euler equations are restored by some estimates, simple like linearisations, or more complex like Roe average velocity for the middle wave speed. HLLC makes it possible to capture phenomena with discontinuities in velocities in the transverse direction and does not add further diffusion where the phenomenon is already characterised by turbulent diffusion in the horizontal plane. The SU2 solver was previously used for application in sonic boom problems, showing promising results[15].

The topology of the computational grid follows a hybrid approach. The mesh is composed by two different parts: an unstructured zone near the aircraft geometry and a structured zone for the remaining domain far from the geometry. The unstructured part is designed as a half cylinder carved into the domain, while the structured part is designed using a blocking technique, as shown in figure 7. The numerical elements are hexahedral in the structured part, tetrahedral in the unstructured zone, and pyramids to connect the two zones. With this approach, the mesh size is around 20 million of elements for the CS1a test case, ensuring a good resolution of pressure perturbation even in the zones far from the aircraft. Starting from operating conditions of table 1, the numerical simulation was performed in the aerodynamic condition of table 2.

Table 2 CS1a Simulation parameters

Operating conditions	Value
Mach number	2.0
Angle of attack [deg]	0
Altitude [m]	15760
Pressure [Pa]	10684.3
Temperature [K]	216.6

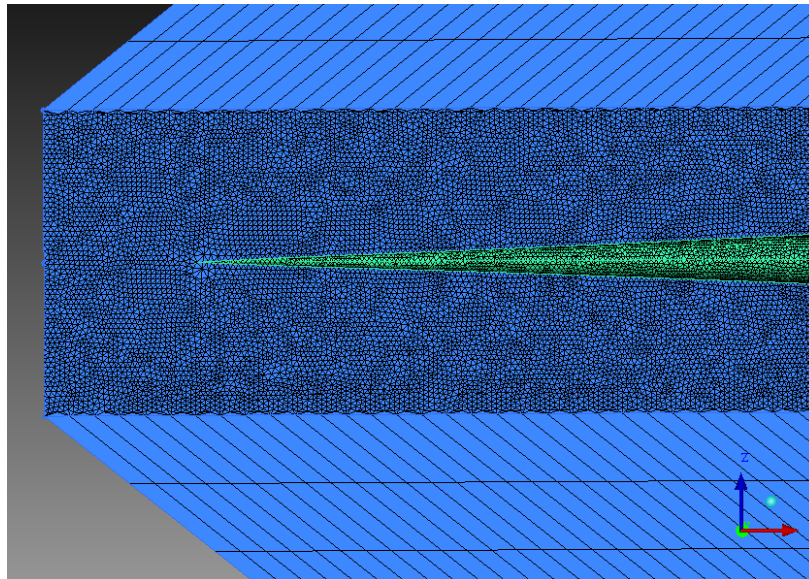


Fig. 7 Detail of hybrid mesh grid for Near-field CFD simulations.

Results of CFD simulation are shown in figure 8. Pressure and Mach number distribution around the aircraft highlight the zones existing shock waves. The resolution of mesh grid consents to retrieve the same aerodynamic field computed around the geometry also in the far-field, ensuring the effectiveness of the numerical procedure employed.

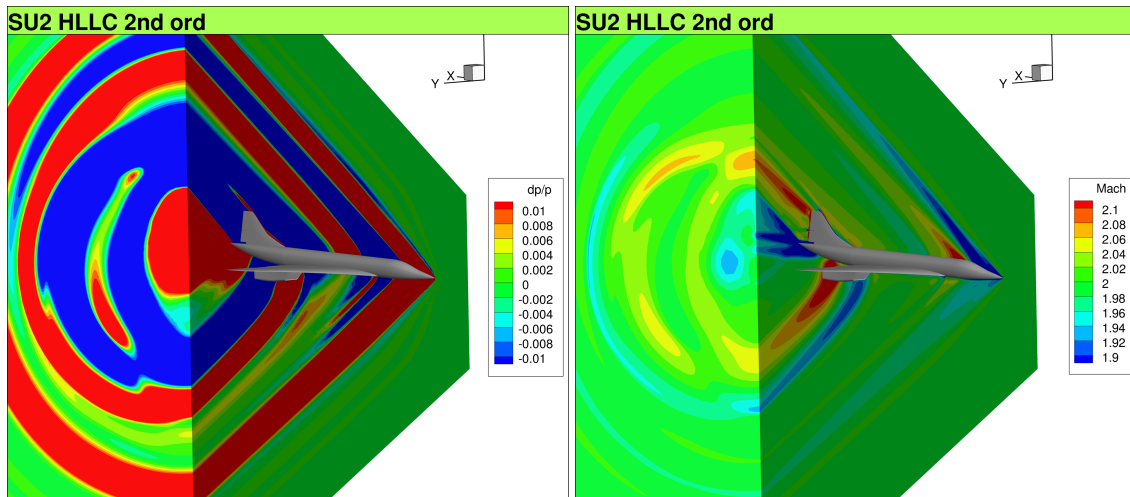


Fig. 8 CS1a contours of pressure field and Mach number from CFD simulations.

Pressure signature in the radial direction around the CS1a geometry, at angles from 0° (under the aircraft) to 180° (above the aircraft), was extracted. In figure 9 are shown the scheme of radial extraction, the pressure signatures and the highest value of noise in decibel computed at each radial angle, i.e. 0° , 30° , 60° , 90° , 120° , 150° , and 180° . Results highlight that there are no big differences in the radial directions. In particular, the pressure signature peaks change from below to upper of the aircraft for each angle. The curve with the greatest values of noise in decibel for each radial angle emphasises this behaviour.

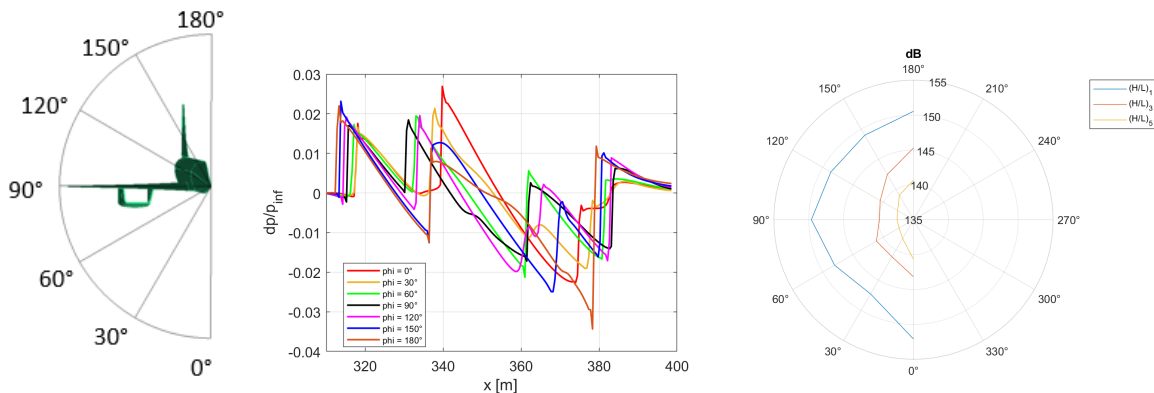


Fig. 9 CS1a radial noise values, pressure signatures and PLdB.

B. Far-field noise Propagation Tool

To simulate the propagation of sonic boom shock waves over long distances towards the ground, another, more detailed far-field propagation algorithm is used to generate comparison results. Unlike the CFD simulation of the turbulent pressure field in the vicinity of the aircraft, as described in the previous chapter, the propagation tool neglects wave refraction but accounts for the inhomogeneities of the atmosphere.

A software for simulating such far-field propagation was developed at the Institute of Air Transportation Systems in Hamburg under the name "propaBoom" [16]. It was validated in comparison to the published results of the Third Sonic Boom Prediction Workshop [17].

This software is based on the Augmented Burgers Equation derived for sonic boom propagation [18]. The Augmented Burgers Equation is a 1-D nonlinear wave equation, which is evaluated on the 1-dimensional domain of an acoustic ray. Acoustic rays must be determined beforehand using linear principles [19]. With the Augmented Burgers Equation, the code can propagate shock waves from sonic boom along acoustic rays and accounts for stratified atmospheric profiles of pressure, temperature, wind, and relative humidity.

For this study, a windless atmosphere with zero relative humidity is assumed. To further match the assumptions of the simplified approach, the temperature and pressure profiles of the ICAO Standard Atmosphere [20] are used. The flight altitude is set to 15760 m, and the Mach number is 2.

From the results of the CFD computations of the local pressure field close to the aircraft, over-pressure signatures are extracted on lines parallel to the aircraft. The position of these lines is determined by the azimuth angle ϕ and the radial distance H . To receive a pressure signature of the shock wave, which is suitable for propagation, a slight fading out is added to the end of the signatures to make them return to zero. Additional zeros are added before propagation, which is also known as zero-padding.

In Figure 10, the raw extracted, as well as the edited, zero-padded near-field signatures are shown. The signatures were extracted at different radial distances H of 1, 3, and 5 times the airplane length L at an azimuth angle of 0° , which is the on-track direction directly below the airplane. The dashed lines show the original parts of the signatures, which do not return to zero, while the solid lines show the edited signatures, which are returning to zero at the end of the signal.

The influence of non-linear propagation between $H/L = 1$ and $H/L = 5$ is visible. Positive shocks are moving towards the beginning of the signal, while negative shocks are moving towards the end of the signal.

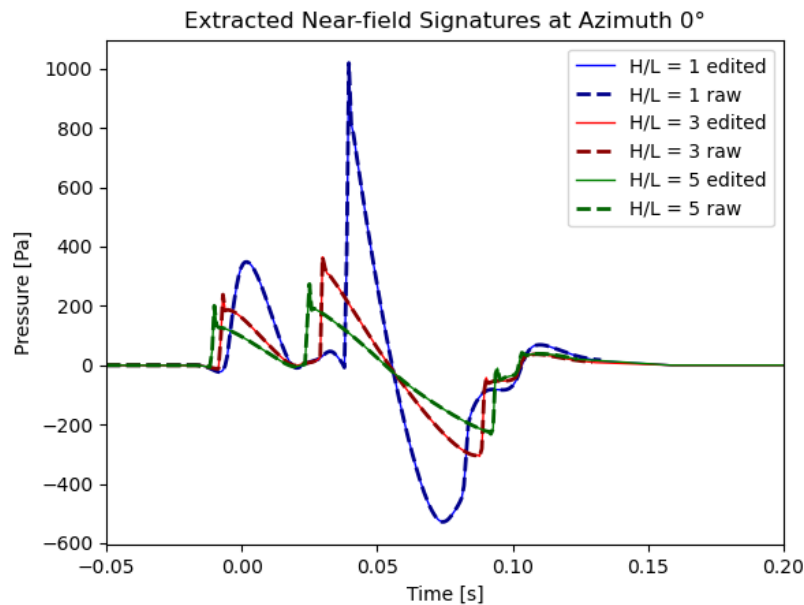


Fig. 10 Extracted on-track (azimuth= 0°) over-pressure signatures at different radial distances from the aircraft

The result of propagating the edited near field signatures with a sampling frequency of 100 kHz and a ray step size of 0.1 seconds or less towards the ground with "propaBoom" is shown in Figure 11. A ground reflection factor of 2 is assumed, to match the assumptions of the simplified methodology study.

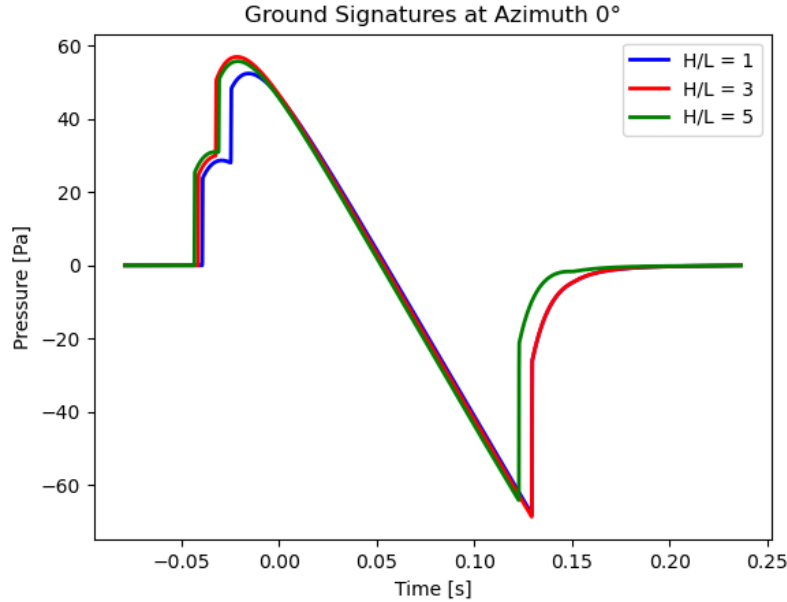


Fig. 11 Computed on-track (azimuth=0°) over-pressure ground signatures for different radial distances of signature extraction

The results for the three different radial distances to extract the signature and start propagation are similar. The classical "N-wave" character of the sonic boom on ground can be observed. Small deviations between the different radial distances are visible in the position of the bow and aft shock.

When choosing the radial distance, it should be considered, that smaller distances mean, that refraction effects of the near-field may be neglected, while larger radial distances mean, that the properties of the atmosphere are assumed to be constant over a greater distance. Based on literature and former findings, the radial distance for the comparison was chosen, such that $H/L = 3$. Deviations between the results for $H/L = 3$ and $H/L = 5$ are visible in the aft shock, where CFD results had to be edited.

VI. Results

The following section shows the comparison results between the simplified methodology and high-fidelity models. In particular, comparisons are represented concerning:

- 1) Ground intersection comparison
- 2) Bow shock overpressure
- 3) Time signature duration

As already mentioned, the reference value of the extraction of pressure values from CFD for the last two graphs is at a $H/L = 3$ as suggested in the literature.

A. Ground Intersection Comparison

For ground intersection comparison, both on-track and off-track conditions were studied for azimuth angles up to 50 degrees. Slight differences are noted for the off-track angle at which the cut-off phenomenon occurs: for the simplified methodology, the azimuth angle for which the signal does not reach the ground is about 51.5° , while for the high fidelity methodology, it is 54.89° .

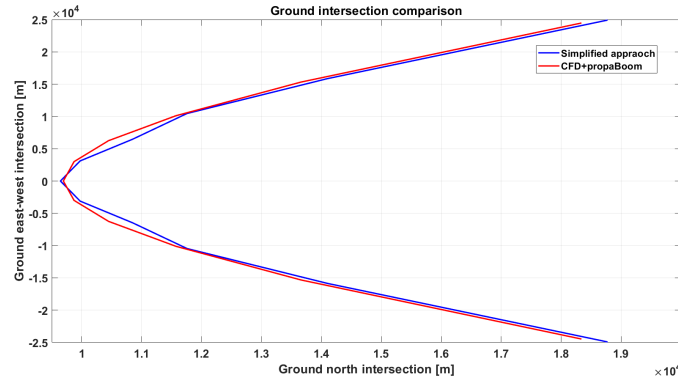


Fig. 12 Comparison in ground intersection between Simplified Approach and propagation tool

Analyzing figure 12 it can be seen that the trend between the two methodologies for angles less than 20 degrees (about 12 km in north intersection) has slight differences, while as the azimuth angle increases these are attenuated.

B. Ground Signature Comparison

The bow shock overpressure value given by the simplified methodology was compared with that given by CFD and propagation tools.

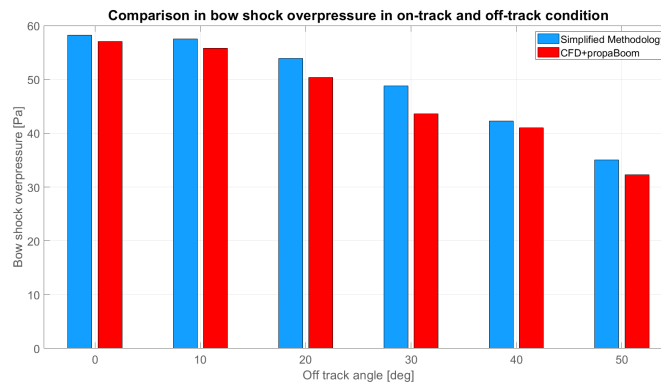


Fig. 13 Bow shock overpressure comparison between Simplified Approach and propagation tool

Table 3 Bow shock comparison

Off track angle [deg]	Simplified methodology [Pa]	High fidelity approach [Pa]
0	58.2	57.04
10	57.53	55.78
20	53.91	50.39
30	48.77	43.61
40	42.23	40.97
50	35.03	32.26

As can be seen from the figure 13 and table 3, the simplified methodology gives slightly higher pressure values than those given by the high-fidelity one. This result provides confirmation, as Carlson's method is conservative by about 5 – 10% from literature [8]. It can be seen that the difference between the two methodologies is very little for low off-track angles, then increases for intermediate angles, until it decreases again for values close to the cut-off value.

C. Time signature duration Comparison

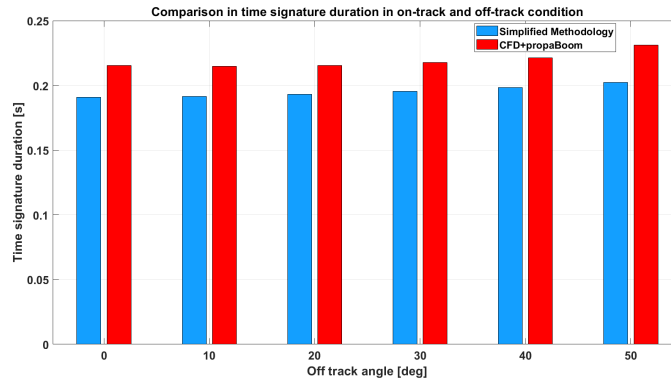


Fig. 14 Time signature duration comparison between Simplified Approach and propagation tool

Table 4 Time signature duration

Off track angle [deg]	Simplified methodology [s]	High fidelity approach [s]
0	0.191	0.21539
10	0.1914	0.21482
20	0.1932	0.21529
30	0.1954	0.21771
40	0.1984	0.22138
50	0.2023	0.23108

As can be seen from figure 14 and table 4, there is in this case a more pronounced difference between the time signature duration provided by the simplified and higher fidelity methodology, however it is within the limit of acceptability for conceptual design.

VII. Conclusion

In the following paper, a comparison was made between a simplifying method applicable to the conceptual design phase and high-fidelity models based on CFD and propagation tools. The comparison was made for an aircraft belonging to the MORE&LESS project with a Concorde-like configuration and similar performance characteristics.

The results show that there is a good correlation between the two methodologies, and the differences are within the limit of acceptability for the conceptual design phase. Furthermore, the entire mission profile in supersonic flight must be carefully studied in the future to evaluate the goodness of the simplifying method for these mission phases as well.

However, there is also a need to study a simplified methodology that imposes fewer constraints than the one used in this paper, and that can be included in a design framework for the future generation of sustainable supersonic aircraft.

References

- [1] Whitham, G., "The Flow Pattern of a Supersonic Projectile," *Communications on Pure and Applied Mathematics*, 1952. <https://doi.org/https://doi.org/10.1002/cpa.3160050305>.
- [2] Seebass, R., "Sonic Boom Theory," *Journal of Aircraft*, 1969. <https://doi.org/https://doi.org/10.2514/3.44032>.
- [3] Seebass, R., "Minimum Sonic Boom Shock strength and Overpressures," *Nature*, 1969. <https://doi.org/https://doi.org/10.1038/221651a0>.
- [4] Seebass, R., and George, A., "Sonic Boom Minimization," *The Journal of Acoustical Society of America*, 1972. <https://doi.org/https://doi.org/10.1121/1.1912902>.

- [5] Hayes, W., and Runyan, H., “Sonic Boom Propagation Through a Stratified Atmosphere,” *The Journal of Acoustic Society of America*, 1972.
- [6] Hayes, W., and Runyan, H., “Effects of atmospheric Irregularities on Sonic Boom Propagation,” *The Journal of Acoustic Society of America*, 1972. <https://doi.org/https://doi.org/10.1121/1.1912904>.
- [7] Plotkin, K., “State of the art of Sonic Boom Modelling,” *The Journal of Acoustic Society of America*, 2002. <https://doi.org/https://doi.org/10.1121/1.1379075>.
- [8] Carlson, H. W., “Simplified sonic-boom prediction,” Tech. rep., 1978.
- [9] Plotkin, K. J., “A Rapid Method for the Computation of Sonic Booms,” *15th AIAA Aeroacoustics COference*, 1993. <https://doi.org/https://doi.org/10.2514/6.1993-4433>.
- [10] Park, M., and Morgenstern, J., “Summary and Statistical Analysis of the First AIAA Sonic Boom Prediction Workshop,” 2014. <https://doi.org/10.2514/6.2014-2006>.
- [11] Park, M. A., and Nemec, M., “Nearfield Summary and Statistical Analysis of the Second AIAA Sonic Boom Prediction Workshop,” *Journal of Aircraft*, Vol. 56, No. 3, 2019, pp. 851–875. <https://doi.org/10.2514/1.C034866>.
- [12] Park, M. A., and Carter, M. B., “Nearfield Summary and Analysis of the Third AIAA Sonic Boom Prediction Workshop C608 Low Boom Demonstrator,” 2021. <https://doi.org/10.2514/6.2021-0345>.
- [13] T. D. Economon, e. a., “SU2: An Open-Source Suite for Multiphysics Simulation and Design,” *AIAA Journal*, 2016. <https://doi.org/10.2514/1.J053813>.
- [14] E.F. Toro, M. S., “Restoration of the contact surface in the HLL-Riemann solver,” *Shock Waves*, Vol. 4, No. 4, 1994, pp. 25–34. <https://doi.org/10.1007/BF01414629>.
- [15] F. Palacios, e. a., “Stanford-Onera-INRIA contribution,” *1st AIAA Sonic Boom Prediction Workshop*, National Harbour-MA, 2014.
- [16] Jäschke, J. J., Liebhardt, B., and Gollnick, V., “Implementation of a Sonic Boom Propagation Algorithm with the Augmented Burgers Equation [Paper presentation],” *Meeting of the Acoustical Society of America, Denver, CO*, Vol. 182, May 24, 2022.
- [17] Rallabhandi, S. K., and Loubeau, A., “Summary of Propagation Cases of the Third AIAA Sonic Boom Prediction Workshop,” *Journal of Aircraft*, 2021, pp. 1–17. <https://doi.org/10.2514/1.C036327>.
- [18] Rallabhandi, S. K., “Advanced Sonic Boom Prediction Using the Augmented Burgers Equation,” *Journal of Aircraft*, Vol. 48, No. 4, 2011, pp. 1245–1253. <https://doi.org/10.2514/1.C031248>.
- [19] Yamamoto, M., Hashimoto, A., Aoyama, T., and Sakai, T., “A unified approach to an augmented Burgers equation for the propagation of sonic booms,” *The Journal of the Acoustical Society of America*, Vol. 137, No. 4, 2015, pp. 1857–1866. <https://doi.org/10.1121/1.4916833>.
- [20] *Manual of the ICAO standard atmosphere: Extended to 80 kilometres (262 500 feet) = Manuel de l’atmosphère type OACI : élargie jusqu’à 80 kilomètres (262 500 pieds) = Manual de la atmosfera tipo de la OACI : ampliada hasta 80 kilómetros (262 500 pies)*, 3rd ed., ICAO, Montreal, 2002.